Hydrological effects on gravity and correlations between gravitational variations and level of the Alzette River at the station of Walferdange, Luxembourg

C. Lampitelli, O. Francis

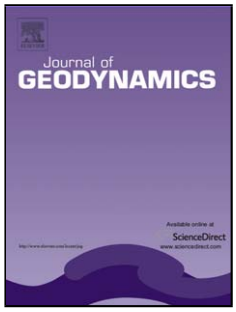

Title: Hydrological effects on gravity and correlations between gravitational variations and level of the Alzette River at the station of Walferdange, Luxembourg

Authors: C. Lampitelli, O. Francis

PII: S0264-3707(09)00066-0
DOI: doi:10.1016/j.jog.2009.08.003
Reference: GEOD 893

To appear in: *Journal of Geodynamics*

Received date: 6-3-2009
Revised date: 21-8-2009
Accepted date: 27-8-2009

Please cite this article as: Lampitelli, C., Francis, O., Hydrological effects on gravity and correlations between gravitational variations and level of the Alzette River at the station of Walferdange, Luxembourg, *Journal of Geodynamics* (2008), doi:10.1016/j.jog.2009.08.003

Hydrological effects on gravity and correlations between gravitational variations and level of the Alzette River at the station of Walferdange, Luxembourg

C.Lampitelli (carmine.lampitelli@uni.lu) and O.Francis (olivier.francis@uni.lu)

Faculty of Science, Technology and Communication. University of Luxembourg

Abstract

The gravitational effects of water storage variations driven by local precipitation events are modeled for the Walferdange Underground Laboratory for Geodynamics (WULG) in the Grand Duchy of Luxembourg. A modified mass continuity model is implemented, which uses rainfall data from Walferdange as input. In the absence of soil moisture and groundwater level information, the model is empirically parameterized. Model outputs are compared to the gravity time series registered with the Observatory Superconducting Gravimeter CT040 located in the WULG. We find that the model explains 77% of the gravity residuals. In addition, a statistical analysis is carried out to determine the relationship between precipitation, gravity variations and water level changes in the nearby Alzette River. A time delay of 88±34 min between the maximum variation rates of the water level and gravity signal has been calculated. The signals have an admittance of 45±5 cm μGal^{-1}.

Keywords: Gravity and Superconducting gravimeter, Hydrology, Groundwater, Precipitation

24 ----------

25 **1. Introduction**

26 The effect of water storage variations on gravity has become an important issue for
27 improving the investigation of gravity measurements. Specifically, local water storage
28 variations within 10 km of a station alter the local mass field and thus can significantly
29 affect gravity observations [*Van Camp et al,* 2006]. Various authors have analyzed the
30 effects of parameters such as local precipitation, soil moisture and groundwater storage
31 on gravity observations [e.g. *Meurers et al., 2007*; *Van Camp et al., 2006; Kroner and*
32 *Jahr,* 2006*; Bower and Courtier,* 1998*; Boy and Hinderer,* 2006*; Kroner,* 2001*; Peter et*
33 *al.,* 1995*; Harnish and Harnish,* 2002*; Crossley and Xu,* 1998*; Imanishi et al.,* 2004;
34 *Llubes et al.,* 2004; *Delcourt-Honorez,* 1989]. Other authors [*van Dam et al.,* 2001*;*
35 *Crossley et al.,* 2005; *Hinderer et al.,* 2006; *Naujoks et al.* 2007] have investigated the
36 consequences of longer wavelength (several 100 km) water storage components on the
37 gravity signal. At these wavelengths, the displacement of the Earth's surface due to the
38 excess mass is also important.

39 The response of local gravity to local changes in water storage is site dependent
40 [*Hokkanen et al.* 2005]. Techniques and schemes for mitigating the signal in gravity data
41 at one location are usually not entirely applicable to another location. In this study, we
42 look at the physical relationship between water storage variations driven by local
43 precipitation events and local gravity changes at Walferdange, in the Grand Duchy of
44 Luxembourg. For the gravity observations, we use the data collected by the
45 superconducting gravimeter CT040 (SG) located in the Walferdange Underground
46 Laboratory for Geodynamics (WULG).

47 The present paper builds on the results of previous authors who have also investigated
48 the correspondence between gravity and local water storage variations. A new and simple
49 scheme is provided to remove the effects of precipitation events in the gravity
50 observations. A synthesis of the different approaches that can be found in recent literature
51 is proposed. The model is then extended to the Walferdange case by including a new
52 parameter to take into account the seasonal variability of groundwater behavior.

53 An empirical model is developed, based on a modification of the basic mass continuity
54 model, to estimate water storage variations due to local precipitation [*Meurers et al.*,
55 *2007*]. This model is used to correct the gravity time series residuals of the
56 superconducting gravimeter. A statistical analysis is then undertaken to determine the
57 correlation between gravity variations registered by the SG and water level changes in the
58 nearby Alzette River.

59 In Sections 2 and 3, a synthetic description of the hydrological recharge and discharge
60 processes related to the water cycle is given. Here the hypotheses leading to a tank model
61 representation are described. In order to underline the dependence of the model
62 parameters on hydrological parameters, such as porosity and hydraulic conductivity, as
63 indicated by *Van Camp et al*. [2006], the steps leading to the fundamental model
64 equations are detailed. This is achieved by combining the mass continuity equation and
65 Darcy's law [*Fetter*, 2001; *Roche*, 1963], which describes the flow of a fluid through a
66 porous medium.

67 In Section 4, modeled gravity variations are estimated using an admittance factor
68 between the gravity change and the precipitation height. This is done by decomposing the
69 area above the gravimeter in a discrete number of prismatic elements (the precipitation

height corresponding to the element thickness). The gravity effect on the SG is calculated using Newton's law of universal attraction. A further hypothesis is developed, regarding the seasonal variability of a model parameter, which represents the gravity recovery rate after a rainfall and its physical significance is discussed.

In Section 5, the model outputs for a set of empirically evaluated parameters are presented and discussed.

In Section 6, a statistical analysis is presented to determine the correlation between the gravity signal variations registered by the SG and the water level of the Alzette River. The gravity variation due to the precipitation should appear before the change in river level. The gravity observation should also contain information on the degree of soil saturation. Understanding the relationship and temporal dependence between the observed precipitation and the gravity changes might improve our ability to predict of extreme events like flooding. We estimate the mean time delay between the maximum variation of the gravity signal and the Alzette water level as a function of a set of sampled showers. Finally, the correlation between the gravity variation and water level variation is calculated and discussed.

2. Hydrological recharge and discharge processes

Variations in the amount of water stored in the ground exert an effect on the gravity signal through essentially two different mechanisms: 1) the Newtonian attraction exerted by the water mass and 2) the ground deformation resulting from the water load and the associated mass redistribution. The effect of the ground deformation on gravity is a long wavelength effect (> 50 km).

Groundwater flow is possible because Earth materials are usually not impermeable, but characterized by the presence of voids (pores) included in a solid matrix. The groundwater and soil moisture occur in the voids [*Fetter,* 2001]. For a control volume V_t of a given material, the porosity P is defined as the ratio between the volume V_v of the voids and the control volume V_t:

$$P = \frac{V_v}{V_t} \tag{1}$$

If the voids are completely/partially filled with water, the medium is defined as saturated/unsaturated.

The mechanical energy per unit weight possessed by a fluid is given by Bernoulli's law:

$$h = \frac{v^2}{2 \cdot g} + z + \frac{p}{\rho \cdot g} \tag{2}$$

where v is the fluid velocity, g is the gravity acceleration, z is the elevation of the fluid center of mass with respect to a reference level, p is the pressure, ρ is the fluid density and h, expressed in units of length, is defined as the hydraulic head. The kinetic term $v^2/2g$ is generally negligible in problems related to groundwater flow [*Fetter, 2001*].

The flow through a porous medium is described by Darcy's law:

$$q = K \cdot (\frac{dh}{dl}) \quad (3)$$

where q (length/time) is the flow per surface unit or specific flow, h is the hydraulic head. and l is the displacement in the flow direction. The proportionality coefficient (K) between the specific flow and the hydraulic gradient (dh/dl) quantifies the capacity of fluids to move through porous media. The coefficient is known as the hydraulic conductivity or permeability coefficient. It is important to underline that hydraulic conductivity is a function of the characteristics of both the fluid and the porous medium [*Fetter,* 2001]. The general formulation of problems related to groundwater flow is based on a combination of Darcy's law and continuity equations with reference to control volumes [*Anderson,* 2007].

For unconfined aquifers the water table represents the interface between the saturated zone (below) and the unsaturated zone (above) [*Milly and Shmakin, 2002*]. The water volume contained in the saturated zone represents the groundwater reservoir. When precipitation occurs, part of the fallen volume of water is retained by the vegetation canopy or human artifacts, another part is subject to direct surface runoff or other subsurface flow, and one part infiltrates through the unsaturated zone to increase the groundwater reservoir storage. This infiltration represents the recharge process, with augmentation of the water storage. After the precipitation event and the recharge process, the stored water will decrease through different mechanisms, such as evaporation and evapotranspiration from the unsaturated zone or efflux through filtration from the saturated zone, to reach draining flows. This represents the discharge process, with consequent diminution of the water storage. In conclusion, both the recharge and the

discharge must be seen as the superposition of different processes with different characteristic time scales. The number of parameters needed to describe those processes is very high, and are subject to strong time and space variability. Different models have been proposed to analyze the complex processes related to water (and energy) storage [*Manabe, 1969; Milly and Shmakin,* 2002, *Iffly et al*., 2004]. In the absence of direct information about soil moisture and groundwater level, the development of an empirical local model is required to describe the water storage variations. Important simplifications of the processes involved are necessary.

3. The Tank Model

The fraction of precipitation that infiltrates the soil, percolates vertically through the unsaturated zone to reach the saturated zone below the water table. This process increases the groundwater reservoir storage. In the case of unconfined aquifers (presence of one impermeable underlying layer), the efflux from the saturated zone can essentially be described as horizontal filtration through a porous medium. The tank model [*Roche, 1963*] represents a strong simplification: the discharge process is reduced to the efflux of water contained in a tank (and not distributed in a solid matrix) through a porous plug. A simple illustration of the tank model is given in Figure 1.

Figure 1

The relation between the flux from the porous plug and the hydraulic head is expressed by Darcy's law (Eq. (3)) in the following form [*Roche, 1963*]:

$$Q = K \cdot \frac{s}{L} \cdot h \quad (4)$$

where Q represents the outgoing flux (volume/time), h is the water height (corresponding to the hydraulic head), s and L are the cross section and length of the plug, respectively (Figure 1). The parameters of the model have to be determined empirically. The outgoing flux is related to the water level through the hydraulic conductivity, which depends both on hydrological soil parameters, such as the medium's porosity, and on fluid characteristics such as viscosity. A hydrological volume balance is calculated, with reference to the elementary time interval dt:

$$S \cdot dh(t) = -Q(t) \cdot dt + S \cdot r(t) \cdot dt \quad (5)$$

where r(t) represents the rainfall rate (length/time) and S the tank surface. Defining the level decrease rate, c (1/time), by:

$$c = \frac{K \cdot s}{S \cdot L} \quad (6)$$

Substituting the definition of Q (Eq. (4)) into Eq. (5), the differential equation describing the water level variation becomes:

$$\frac{dh(t)}{dt} = -c \cdot h(t) + r(t) \quad (7)$$

Equation (7) relates the water level, corresponding to the hydraulic head in this simplified representation, to the rainfall. In this equation, r(t) is not a continuous function of time and the integration has to be performed numerically. In absence of precipitation, the equation can be analytically integrated leading to an exponential decay expression describing the draining of a tank through a porous plug.

4. Relation between precipitation height and gravity variation

The WULG is located underground in a derelict gypsum mine, at latitude 40.6700°N, longitude 6.1500°E. The laboratory housing the Observatory Superconducting Gravimeter *CT040* lies at the end of an 800 m long tunnel cut into the side of a ridge. The gravity sensor is 295 m above sea level and about 80 m below the local surface. The area above the gravimeter has significant topographic slope gradients (See Figure 2), and is covered by uneven vegetation. The closest human artifacts (i.e. roads and buildings) are located at about 500 m from the gravimeter. All of these factors contribute to making the WULG seismically quiet.

In order to express Eq.(7) in terms of gravity variations, we estimate the admittance between the gravity change and the precipitation height. The gravity effect of a weathered area can be calculated using digital elevation models (DEM): the weathered ground layer is discretized in prismatic elements [*Van Camp et al., 2006; Banerjee and Das Gupta, 1977; Talwani, 1973*]. The gravity effect Δg_e of a single element is given by:

$$\Delta g_e = G \cdot \rho_{wet} \cdot \int_{x_1}^{x_2}\int_{y_1}^{y_2}\int_{z_1}^{z_2} \frac{z}{(x^2+y^2+z^2)^{3/2}} \cdot dx \cdot dy \cdot dz \qquad (8)$$

where G is the Newtonian universal constant of gravity ($6.67428 \cdot 10^{-11}$ m^3 kg^{-1} s^{-2}) and ρ_{wet} is the density of the wet component of the weathered zone (mass/volume). The integration is carried out over the prism volume, delimited by the coordinates (x_1, y_1, z_1) and (x_2, y_2, z_2) in a Cartesian frame centered at the gravity station.

In absence of accurate information about ρ_{wet} in the weathered zone above the WULG, the calculation is made directly on prismatic water elements having the precipitation height as thickness. This simplification is adopted because the thickness of the weathered zone appears to be significantly smaller than the distance between the gravity sensor and the surface.

The 2000 m x 2000 m zone above the gravimeter is divided into 10000 prismatic elements of size 20 m x 20 m. The map projection of the discretized layer defines a 100 x 100 grid. The square elements of the grid are identified by the indices i and j corresponding to the coordinates in meters x_i=20i, y_j=20j and elevation z_{ij} in a local Cartesian frame (the coordinates are referred to the element central points). The gravimeter is located at (x_g, y_g, z_g). The gravity effect Δg_{ij} of each prism (m s^{-2}) at the gravimeter location is calculated with:

$$\Delta g_{ij} = G \cdot \Delta S \cdot \rho \cdot l_e \cdot \frac{z_{ij}}{((x_i - x_g)^2 + (y_j - y_g)^2 + (z_{ij} - z_g)^2)^{3/2}} \quad (9)$$

where ΔS is the surface area of the element (400 m^2), ρ represents the water density (1000 kg m^{-3}) and l_e is the element thickness (m). The total gravity effect Δg of the layer (m s^{-2}) on the gravity sensor is given by:

$$\Delta g = \sum_{i=1}^{100}\sum_{j=1}^{100} G \cdot \Delta S \cdot \rho \cdot l_e \cdot \frac{z_{ij}}{((x_i - x_g)^2 + (y_j - y_g)^2 + (z_{ij} - z_g)^2)^{3/2}} \quad (10)$$

The admittance, α, between a gravity change (μGal) and a precipitation height (m) is directly calculated with Eq.(10), by defining l_e=1 m and expressing the gravity in μGal. The result is α=36 μGal m^{-1}. For reference, the value given by the Bouguer infinite plate model is 42 μGal m^{-1}. This value is generally adopted for almost flat surfaces. The significant height differences of the area above the WULG justify the calculation made on the actual topography.

Figure 2

With the calculation of the admittance between the hydrological component of the gravity variation and the precipitation height, the equation describing the gravity changes can be obtained by writing the continuity equation (7) in terms of gravity. This is done by multiplying both sides of Eq.(7) by α, setting Δg=α·h, c=γ, and changing the sign of the term α·r. This last step is required by the fact that the gravimeter is located in an underground laboratory: an increase of the stored water level above the gravimeter will produce a reduction of the gravity signal. We thus obtain:

$$\frac{d(\Delta g)}{dt} = -\gamma(t) \cdot \Delta g - \alpha \cdot r(t) \quad (11)$$

where Δg represents the hydrological part of the gravity variation and γ (corresponding to c in Eq.(7)) is here defined as the gravity recovery rate after rainfall (1/time). The coefficient γ is related to hydrological parameters like hydraulic conductivity and porosity, in addition to the geometrical parameters depending on the local configuration. The inverse of γ, defined as τ, has the dimensions of a time and it characterizes the duration of the discharge phase. Equation (11) has been previously implemented by *Imanishi et al.* [2004] to calculate the gravity effects of underground water in Matsushiro (Japan). The basic tank model is modified using the hypothesis of a seasonal variability for the parameter γ. The seasonality is included to account for the annual changes in the meteorological and hydro geological conditions (i.e. evapotranspiration and hydraulic conductivity). This variability is expressed in the form:

$$\gamma(t) = \gamma_0 \cdot (1 + A \cdot \cos(\frac{2 \cdot \pi}{T} \cdot t + \varphi)) \tag{12}$$

where γ_o is the mean value of γ in the period T (one year). The values of A (amplitude) and φ (phase) are evaluated empirically (see Section 5.2.). Finally, the equation for the gravity variation becomes:

$$\frac{d(\Delta g)}{dt} = -\gamma_0 \cdot (1 + A \cdot \cos(\frac{2 \cdot \pi}{T} \cdot t + \varphi)) \cdot \Delta g - \alpha \cdot r(t) \tag{13}$$

As already pointed out, the rainfall rate r(t) is not defined by a continuous function of time but by a discrete set of values. To allow us to solve the equation using finite

difference algorithms, Eq. (13) has to be rewritten as a discrete expression. We define the terms of a progression:

$$\Delta g(i+1) = (1-\gamma(i)) \cdot \Delta g(i) - \alpha \cdot r(i) \quad (14)$$

where i represents the non dimensional time indices, $\gamma(i)$ is the non dimensional recovery rate and r(i) are the precipitation heights. The time variable t in Eq. (13) is given by $t=\Delta t \cdot i$, where Δt is the reference time interval (1 hour in the hourly implementation), and the recovery rate function $\gamma(i)$ is formally identical to $\gamma(t)$.

5. Data and Results

5. 1. Input Data

The available data for the model implementation are the local rainfall time series from the 1 January 2003 to the 1 January 2009. Two different data sources were available: the pluviometer of the Walferdange Meteorological Station and the WULG pluviometer (Figure 2). Both the pluviometers provide the rainfall heights (mm) at one-minute sampling intervals. A comparison between the two series indicates a qualitative similarity. A significant quantitative difference exists as well. The cumulative precipitation provided by the WULG is approximately 10% greater than the cumulative precipitation provided by the Walferdange Meteorological Station. This difference will be used to assess the uncertainties of the rainfall data. The time series provided by the WULG is displayed in Figure (3).

Figure 3

5. 2. Model parameterization for the hourly implementation

The value of the admittance, α=36 μGal m^{-1}derived in Section 4, has been used for the model parameterization in Eq.(13). The parameters γ_o, A and φ in the same equation are obtained empirically by a least square adjustment. The gravity variations observed with the SG are compared with the values predicted by Eq.(13) using the rainfall data, for the period 19 December 2003 to 1 December 2004. The parameters are determined from the data in order to minimize the residuals. The values of A=0.6, $\varphi = 2\pi/5$, and γ_o=0.0011 $hours^{-1}$ provide the best results. For reference, *Meurers* (2007) adopted the value τ=720 hours for the discharge time parameter at the gravity station in Vienna, which corresponds to γ_o=0.0015 $hours^{-1}$ (see Section 4).

5. 3. Results

The rainfall time series provided by the WULG, integrated to hourly values and referred to the mid-hour points, are used as model input. The rainfall heights are expressed in meters. An uncertainty of 10% on the rainfall data, as determined by the quantitative difference in the rainfall data from two closely space pluviometers (see Section 5.1) is assigned.

The modeled hourly time series of the gravity (μGal) is compared with the observed hourly time series obtained from the SG for the period 19 December 2003 to 1 January 2009. The instrumental drift of the SG is modeled using an exponential function [*Van*

Camp and Francis, 2006]. The modeled gravity (green), the observed gravity (blue) and their difference (red), expressed in μGal, are displayed in Figure 4.a.

Figure 4

The RMS of the uncorrected gravity time series is 1.89 μGal. After removing the modeled hydrological effects from the observations, an RMS value of 0.89 μGal is obtained, which corresponds to a 77% signal reduction.

The gravity changes after a high intensity precipitation event (Figure 4.b) show that the gravity recovery process has a significantly longer duration than the gravity decrease process. The tank model describes only the recovery process. The gravity decrease process is considered as instantaneous. When a precipitation occurs, the rainfall height is simply added to the current water level, producing an instantaneous gravity change. A higher time sampling of the data is therefore not necessary.

5. 4. Discussion

The model provides a reasonable description of the medium and long term effects of rainfall on the gravity observations. However, it does not describe short time scale effects like air pressure changes or air mass redistribution which may themselves be related to the precipitation events [*Meurers, 2007*; *Meurers et al., 2007*]. The hypothesis of the seasonal variability of the gravity recovery rate after rainfall provides a better fit to the actual gravity changes. This variability could be explained from four different factors.

First, it could be due to variability of the hydraulic conductivity K, which is related to the parameter γ [*Van Camp et al., 2006*]. K can be expressed in the form $K=k\cdot\rho\cdot g\cdot\mu^{-1}$, where k (length²) is the permeability of the solid matrix, which depends only on the characteristics of the porous medium. The term $\rho\cdot g\cdot\mu^{-1}$ depends only on the fluid characteristics, where ρ and μ represent the density and the viscosity of the fluid, respectively. The viscosity depends on groundwater temperature. At mid-latitude locations such as Walferdange, groundwater temperature has a definite seasonal variability, even if it is less sensitive in the saturated zone. *Bartolino* (2003) investigated the annual groundwater temperature fluctuations as a function of depth below the surface beneath the Rio Grande in New Mexico. He estimated an annual groundwater temperature range varying from 22°C at 1 m depth below the surface to 4°C at 15 m depth below the surface..

A second seasonal effect which could positively affect our comparison, could be due to the infiltration variability. The runoff coefficients, and consequently the fraction of precipitation infiltrating the soil, can have a significant seasonal variability, related to the degree of saturation of the root zone.

Thirdly, the improvement could be due to evapotranspiration variability [*Hupet and Vanclooster, 2005*]. The process of evapotranspiration has a strong dependence on air and soil surface temperatures that are subjected to significant seasonal oscillations.

Finally, it could be due to regional effects. The model is based on local precipitation. However, the gravity recovery rate variability hypothesis may absorb longer wavelength seasonal effects as well [*van Dam et al., 2001*; *Crossley et al., 2005*].

A confirmation of the variability of parameter γ (ranging from 0.4 γ to 1.6 γ_o as results from Eq. (12) with A=0.6) can be obtained by a comparison with the Antecedent Precipitations Index (API) calculation model [*Musy and Higy*, 2003; *Rosenthal et al.* 1982]. The API relates the soil moisture level to the precipitation via the expression:

$$API_i = API_{i-1} \cdot K_p + P_{i-1} \quad (15)$$

where API_i is the index (mm) at time i, API_{i-1} the index at time i-1, P_{i-1} the precipitation (mm) at time i-1 and K_p is a coefficient <1, that appears strongly correlated to parameter γ in Eq. (11). *Rosenthal et al*. [1982] have estimated that in Washita Basin (USA), for a superficial layer of 15 cm thickness, the value of K_p ranges from 0.84 in July to 0.99 in December. The correlation between γ and K_p indicates that the local value of γ may range from 0.1 γ_o to 1.6 γ_o, where γ_o represents the yearly average value. Implementing the tank model with a constant value of γ, the seasonal variations are not absorbed and the maximum percentage of signal scatter reduction in Walferdange is only 25%.

6. Correlation between gravity variation and level of the Alzette River

In this Section, we determine the statistical correlation between the gravity variations registered by the SG and the water level changes of the Alzette River. The motivation for this analysis is that hydrological gravity may show a better correlation with river water levels than precipitation. This is because both gravity and water level changes are dependent on soil hydrological parameters, whereas rainfall is not.

385 The water level data is available from the Walferdange Meteorological Station 1.63
386 km away and downhill from the WULG (see Figure 2). The direct effect of the water
387 level change on observed gravity variations can be neglected due to the distance between
388 the SG and the river.

389 A shower [*Musy and Higy, 2003*] is defined as an ensemble of precipitation events
390 related to the same meteorological perturbation. Two showers are considered distinct if,
391 during a defined time interval Δt_s the precipitation height is inferior to a defined level
392 Δh_s [*Musy and Higy, 2003*]. The water level increase duration Δt_i is defined as the time
393 delay between the start of river level increase and the maximum river level increase due
394 to a particular shower. The mean water level increase duration $<\Delta t_i>=185\pm35$ min is
395 calculated for 45 showers sampled between January 2004 and April 2007. In general the
396 same value can be adopted for the parameter Δt_s. The value of Δh_s is the minimum
397 continuous precipitation for which a water level increase can be observed. The values of
398 3 hours and 0.5 mm hour^{-1} are adopted for Δt_s and Δh_m, respectively.

399 In addition to Δt_s and Δh_m, defined as continuity parameters, the quantitative
400 parameters characterizing a shower are the duration (time), the precipitation height (mm),
401 the mean intensity, ratio between the precipitation height and the shower duration, and
402 the maximal intensity [*Musy and Higy, 2003*].

403 In this section, the time delay between the gravity and water level variations due to the
404 showers and the correlation between the gravity and water level changes are estimated.

405

406 **6.1. Time delay between gravity and water level variations**

In order to estimate the time delay of gravity and water level variations, it is more precise to work with the time derivative of the quantities. The sampling interval of the water level time series L(t) is 15 min. The time derivative of L(t) is defined as:

$$\dot{L}(t) = \frac{L(t+\Delta t) - L(t)}{\Delta t} \tag{16}$$

The time derivative $\Delta\dot{g}$ (t) of the gravity time series Δg(t) is computed in a similar way. Two additional parameters are defined: t_l is the time delay between the maximum values of the precipitation intensity and the gravity time derivative related to a shower, t_s is the time delay between the maximum values of water level and gravity time derivatives related to a shower (Figure 5).

The statistical analysis is made for 30 showers sampled between January 2005 and February 2007. In general, it is difficult to estimate the time delay between the signals as the relationship can be clearly identified only for some type of showers: high intensity showers and medium intensity showers with their maximum intensity concentrated in the initial phase.

Figure 5 displays the rainfall height (mm), the gravity time derivative (μGal hour^{-1}) and the water level time derivative (cm hour^{-1}) related to the shower, which occurred on the 25 June 2006.

Figure 5

The average values and the standard deviation of t_s calculated for the entire sample, for the showers that occurred in the time span April to September (warm months), and for the showers that occurred in the time span October to March (cold months) are presented in Table 1. No substantial differences appear in the values calculated for the three periods, but because of the sample limitation these results must be interpreted with caution.

Table 1

The average values and the standard deviation of t_l are also calculated for 3 subsets: the entire sample, for the time span April to September (warm months) and the time span October to March (cold months). The results are given in Table 2.

Table 2

As the uncertainties of the t_l values are even greater than the values themselves, the SG observations do not provide any additional or complementary information already provided by the pluviometer.

6.2. Correlation between gravity and water level changes as a function of the shower height

A statistical analysis of the correlation between the shower heights, the gravity variations and the water level changes is carried out for 45 showers sampled between January 2004 and April 2007.

453 The parameters r_s, Δg_s and L_s are defined as the integrated water content of a shower,
454 the gravity change, and the water level change associated with a shower (Figure 6)
455 respectively. The L_s values as a function of the Δg_s values are displayed in Figure 7.
456
457 **Figure 6**
458
459 The correlation coefficient between L_s and Δg_s is 0.59. The admittance between L_s
460 and Δg_s was calculated to 45±5 cm μGal^{-1}
461
462 **Figure 7**
463
464 The L_s values as a function of the r_s values are displayed in Figure 8. The correlation
465 coefficient between L_s and r_s is 0.68, higher than the correlation coefficient between L_s
466 and Δg_s. The admittance of 2.2±0.4 cm mm^{-1} between L_s and r_s is calculated. Again, the
467 slightly better correlation between L_s and r_s shows that the SG observations (as compared
468 to predictions based solely on the pluviometer) fail to provide a better insight into river
469 levels.
470
471 **Figure 8**
472
473 **7. Conclusions**
474 A simple tank model, based on a combination of a mass continuity equation and
475 Darcy's law, is implemented in order to evaluate the effects of water storage variations
476 on the gravity observations in Walferdange. The hypothesis of the seasonal variability

of the model parameter describing the gravity recovery rate after a rainfall is introduced. No a priori information about soil moisture and groundwater storage is used to estimate the hydrological effects on gravity. The model is based solely on the observed local rainfall and is empirically parameterized.

The model reduces the scatter of the SG data by 77%. However, in the absence of the extra seasonal parameter, the maximum percentage of signal reduction is 25%. This result indicates that seasonal effects are important even when looking at short-scale spatial relationships.

The time delay between the maximum gravity and water level time derivatives and maximum precipitation intensity and gravity time derivative is 88±34 minutes and 4±9 minutes, respectively. The correlation between the gravity and water level variation and the precipitation amount and water level variation is 0.59 and 0.68, respectively. The admittance between water level and gravity variation and water level variation and precipitation amount is 45±5 cm μGal^{-1} and 2.2±0.4 cm mm^{-1}, respectively.

In conclusion, the gravity signal does not allow for a better prediction of the water level of the Alzette as compared to the prediction based solely on the pluviometer.

Acknowledgements

We are grateful to Prof. Tonie van Dam for the help she provided in revising the paper and editing the English. Thanks are also due to Dr. Jan Wuite for contributing to improve the paper. The Observatory Superconducting Gravimeter CT040 has been acquired by the University of Luxembourg and the Musée National d'Histoire Naturelle of Luxemburg in the framework of the project Gravilux. The European Center for Geodynamics and

Seismology (ECGS) is providing the funds to maintain and operate the superconducting gravimeter. We are grateful to the two anonymous referees for their constructive and thorough reviews.

References

Anderson M.P. (2007). Introducing groundwater physics, *Physics today, vol. 60, 42-47*.

Banerjee, B. , Das Gupta, S. P. (1977). Gravitational attraction of rectangular parallepiped, *Geophysics, 42, 1053-1055*.

Bartolino, J.R. (2003). Heat as a tool for studying the movement of groundwater near streams, *U.S. Geological Survey circular no. 1260*.

Bower D.N., Courtier N. (1998). Precipitation effects on gravity measurements at the Canadian Absolute Gravity Site, *Physics of the earth and plan, int. 106, 353-369.*

Boy J., Hinderer J. (2006). Study of the of the seasonal gravity signal in superconducting gravimeter data , *J. Geodyn. , 41, 227-233*.

Crossley, D., Xu, S., (1998). Analysis of superconducting gravimeter data from Table Mountain, Colorado. *Geophys. J. Int., 135, 835-844.*

Crossley, D, J., Hinderer, J., Boy, J.-P., (2005). Time variation of the European gravity field from superconducting gravimeters, *Geophys. J. Int.,161, 257-264.*

Delcourt-Honorez M.(1989).Water level fluctuations in a borehole at the Royal Observatory of Belgium: effects on local gravity, Earth-tidal and barometric responses, *XIth international symposium on Earth tides.*

Fetter, C. W., (2001). *Applied hydrogeology*, 4th ed., 598 pp, Prentice-Hall. Upper Saddle River, N. J.

Harnisch M., Harnisch G. (2002). Seasonal variations of hydrological influences on gravity measurements at Wettzell. *B Inf. Marées Terr., 137:10849–10861*.

Hinderer J., Lemoine F., Crossley D., Boy J. (2006). Time changes of the European gravity field from GRACE: a comparison with ground measurements from superconducting gravimeters and with hydrology model predictions, *Geophysical Journal International, Vol. 61 issue 2, 257-264.*

Hokkanen T., Virtanen H., Pirttivaara M. (2005). Hydrogeological noise in superconducting gravimeter data, *Near Surf. Geophys, 5: 125–132.*

Hupet F., Vanclooster M. (2005). Micro-variability of hydrological processes at the maize row scale: implications for soil water content measurements and evapotranspiration estimates, *Journal of Hydrology, Volume 303, Issues 1-4, 247-270.*

Iffly J.- F., Drogue G., El Idrissi A., Hoffman L., Matgen P., Talliez C., Pfister L. (2004). Empirical relationship between rainfall, groundwater level and basin humidity as a tool for predicting peak discharge, *Geoph.Res.Abs., Vol 6, 04489.*

Imanishi Y., Sato T., Higashi T., Sun W., Okubo S. (2004). Submicrogal coseismic gravity changes detected by a network of superconducting gravimeters, *Science, Vol 306, No 5695, 476-478.*

Kroner C., Jahr T. (2006). Hydrological experiments at Moxa observatory, *J. Geodyn.*, 41(1-3), *268-75.*

Kroner C., (2001). Hydrological effects on gravity data of the geodynamic observatory Moxa, *J. Geod. Soc. Jpn., 47(1), 353-358.*

Llubes M., Florsch N., Hinderer J., Longuevergne L. & Amalvict M.**,** (2004). Local hydrology, the Global Geodynamics Project and CHAMP/GRACE perspective: some case studies., *Journal of Geodynamics, 38 :355-374.*

Manabe S., (1969). Climate and ocean circulation. I. The atmospheric circulation and the hydrology of the Earth's surface. *Mon. Wea. Rev*., 97, 739-774.

568 Meurers B. (2007). Long and short term hydrological effects on gravity in Vienna.
569 *www.astro. oma.be.*
570
571 Meurers B., Van Camp M., Petermaans T. (2007). Correcting superconducting time-
572 series using rainfall modeling at the Vienna and Membach stations and application to
573 Earth tide analysis, *J. Geod 81:703-712.*
574
575 Milly P.C.D., Shmakin A.B. (2002). Global Modeling of land water and energy balances,
576 *Journal of Hydrometeorology, vol. 3.*
577
578 Musy A., Higy C. (2003). Hydrologie, *Presses Polytechniques et Universitaires*
579 *Romandes*
580
581 Naujoks M., Weise A., Kroner C., Jahr T.(2007). Detection of small hydrological
582 variations in gravity by repeated observations with relative gravimeters, *J. Geod*
583 *DOI 10.1007 / s00190-007-0202-9, vol. 82[9],543-553.*
584
585 Peter G., Klopping F.J., Berstis K.A. (1995). Observing and modeling gravity changes
586 caused by soil moisture and groundwater table variations with superconducting gra-
587 vimeters in Richmond, Florida, USA, *Cahiers du Centre Européen de Géodyna-*
588 *mique et de Séismogie, Vol 11.*
589
590 Roche M. (1963). Hydrologie de surface, *Gauthier-Villars Orstom, Paris.*
591

592 Rosenthal W.D., Harlan J.C., Blanchard B.J. (1982). Case study: estimating antecedent
593 precipitation index from Heat Capacity Mapping Mission day thermal infrared data.
594 *Hydr. SC. Journal, vol. 7, no 4, déc. 1982, pp. 415-426.*
595
596 Talwani, M.(1973) Computer usage in the computation of gravity anomalies, Academic
597 Press.
598
599 Van Camp M., Francis O. (2006). Is the instrumental drift of superconducting
600 gravimeters a linear or exponential function of time?, *J. Geod. 81:337-334.*
601
602 Van Camp M., Vanclooster M., Crommen O., Petermans T.,Verbeek K., Meurers B., van
603 Dam T.,Dassargues A. (2006). Hydrological investigations at the Membach
604 station, Belgium, and applications to correct long periodic gravity variations,
605 *J.Geoph. Res. Vol.111, BI0403.*

606 van Dam, T., Wahr, J., Milly, C., and Francis, O., (2001). Gravity Changes due to
607 Continental Water Storage , *J. Geod. Soc. Japan.*

608

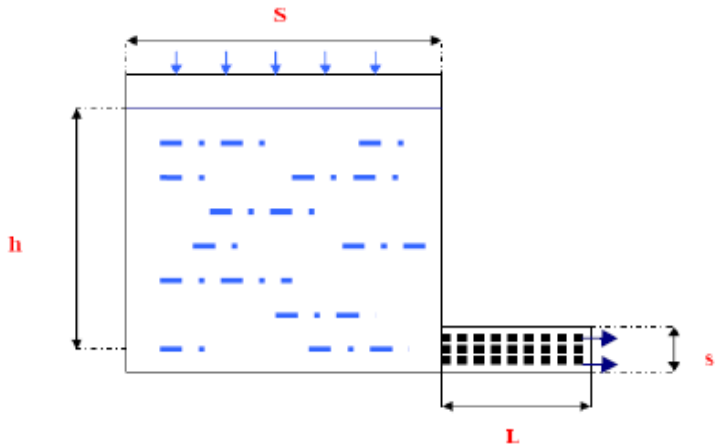

Fig. 1: *The tank model: S is the tank surface, h the water level, s and L the cross section and length of the plug..*

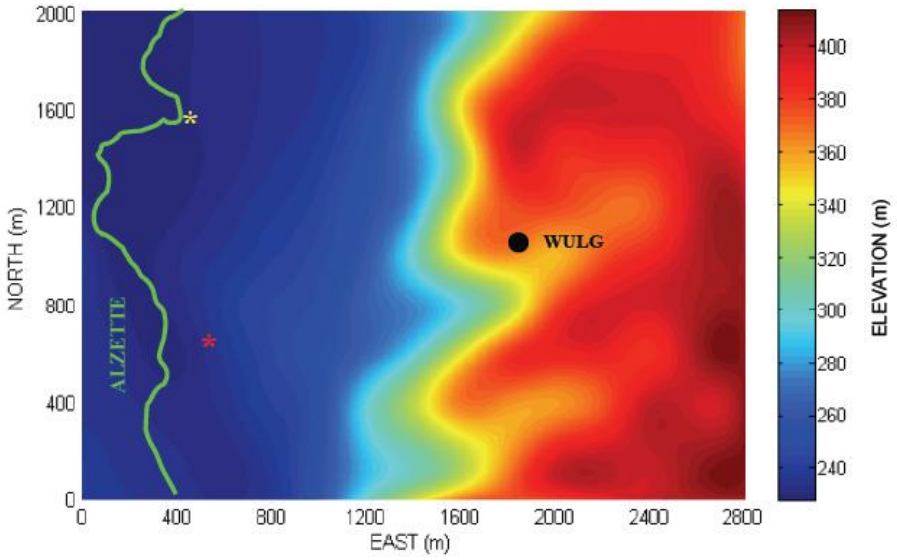

***Fig. 2**: Topography of the area above the WULG (black dot) and Alzette River (green line). The red asterisk represents the WULG pluviometer. The yellow asterisk represents the Walferdange Meteorological Station.*

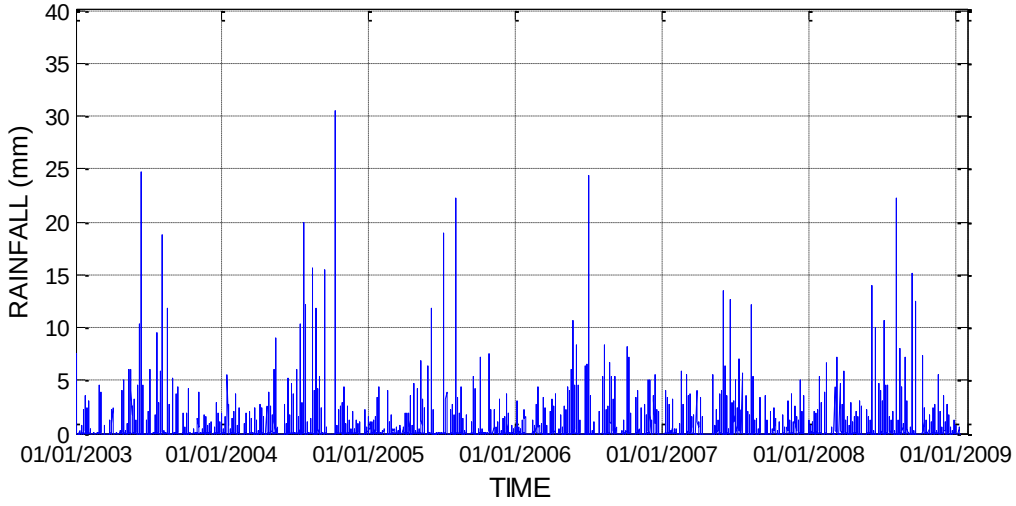

***Fig. 3**: Input data: Rainfall time series (mm/hour) provided by the WULG for the period 1 January 2003 to 1 January 2009.*

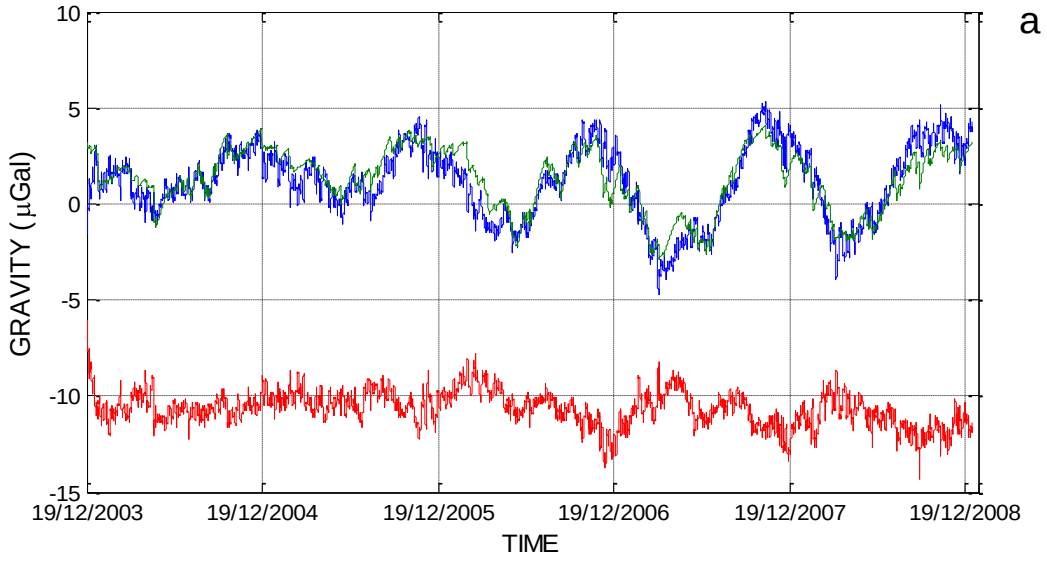

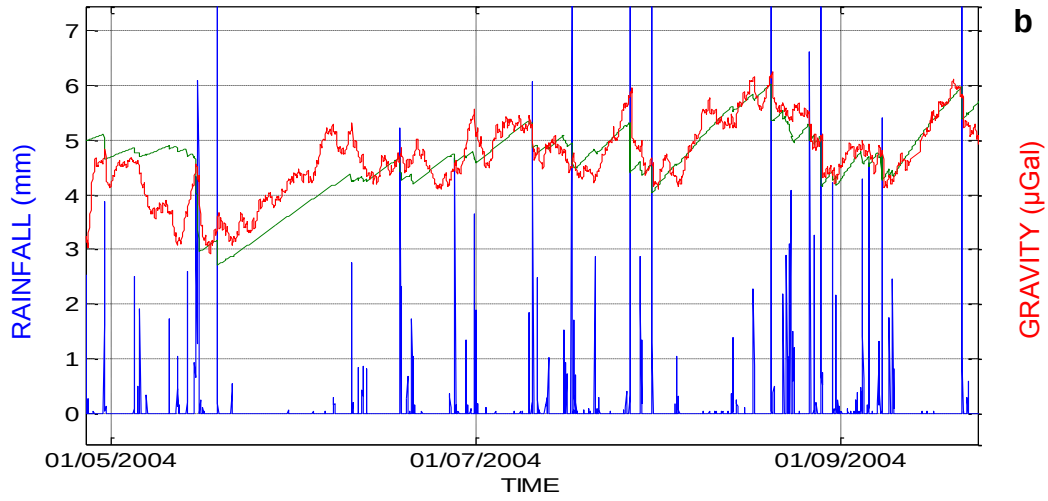

***Fig. 4**: Model outputs:*

a. Observed gravity (blue, µGal), modeled gravity (green, µGal) and their difference (red, µGal) at Walferdange. The comparison period is 19 December 2003 to 1 January 2009.

b. Zoom on a: rainfall (blue, mm/hour), observed gravity (red, µGal), modeled gravity (green, µGal) for the period May to September 2004. The same scale is adopted for gravity and rainfall.

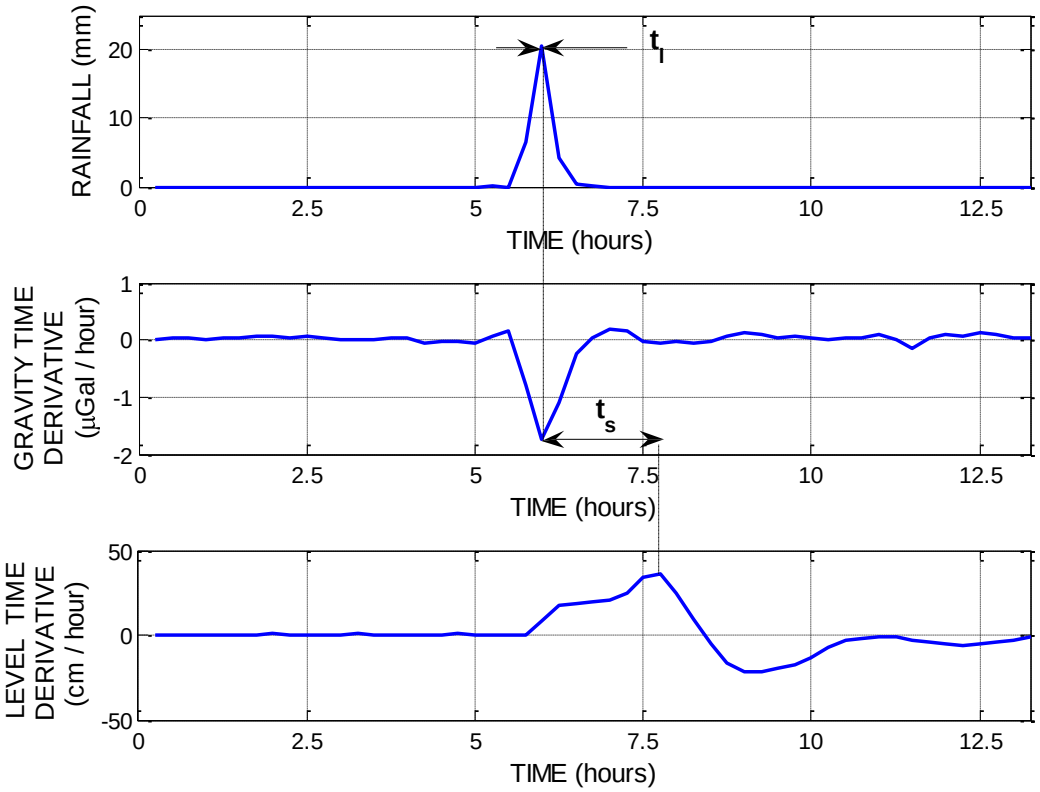

***Fig. 5**: Rainfall height (mm), gravity time derivative (μGal/hour) and water level time derivative (cm/hour) related to the shower that occurred on the 25 June 2006.*

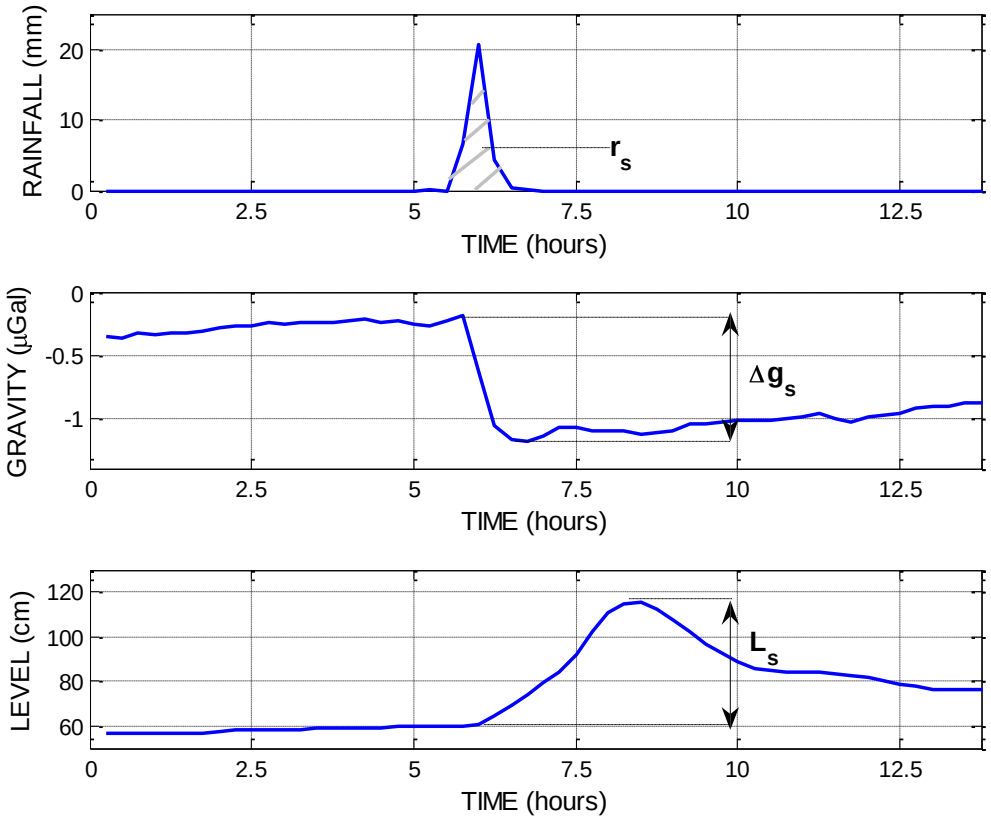

Fig. 6: *Time evolution of rainfall (mm), gravity (μGal) and water level (cm) related to the shower that occurred on the 25 June 2006.*

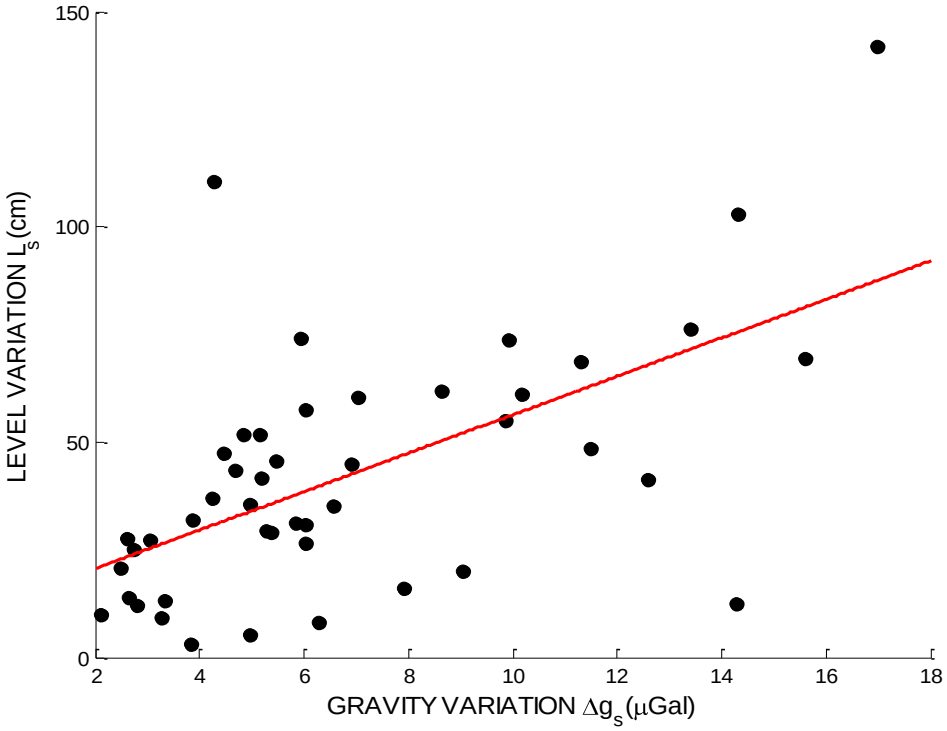

***Fig. 7**: Correlation between gravity and water level changes for the showers between January 2004 and April 2007.*

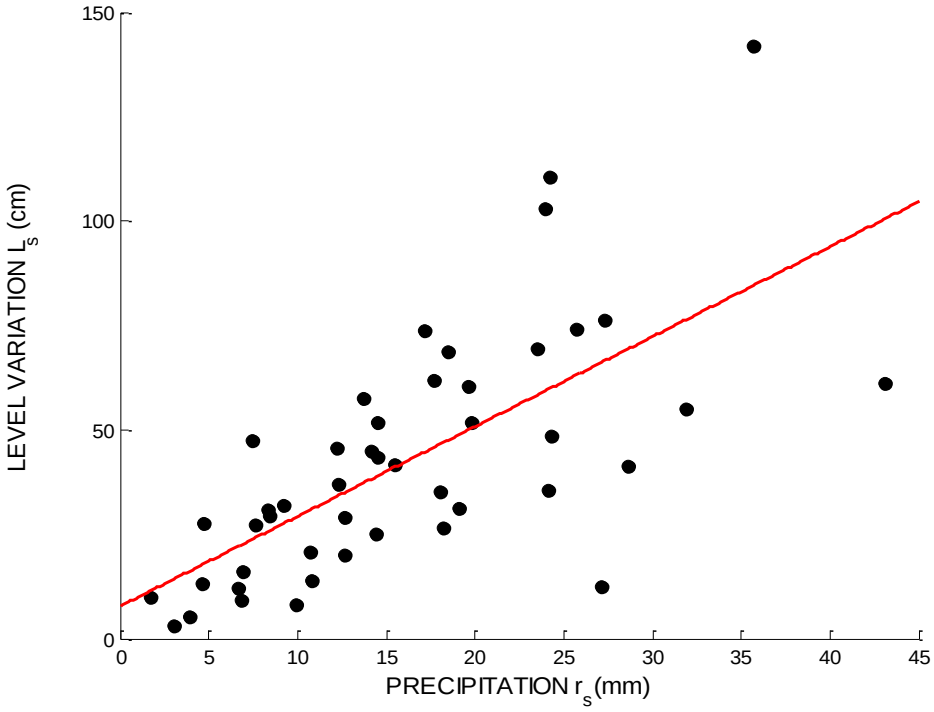

***Fig. 8**: Correlation between precipitation heights and water level changes for the showers between January 2004 and April 2007.*

	January 2005-February 2007	April-September 2005-2007	October-March 2005-2007
$\mathbf{t_s}$	88 ±34 min	85±34 min	93 ±34 min

***Table 1**: Time delay t_s between the maximum values of gravity and water level time derivatives, for the showers sampled between January 2005 and February 2007.*

	January 2005-February 2007	April-September 2005-2007	October-March 2005-2007
$\mathbf{t_l}$	4±9 min	5 ±9min	1 ±9 min

***Table 2**: Time delay t_l between the maximum values of shower intensity and gravity time derivative, for the showers sampled between January 2005 and February 2007.*